# Study of the Corrosion behavior of de $TiO_2/CeO_2$ coating on Ti6Al4V alloy

Edgar ONOFRE B.[1], Greta de M. TAVAREZ M.[1], Edna C. DE LA CRUZ T.[2], Adriana MONTIEL G.[1] María ESCUDERO R.[3], Juan Pablo LEÓN G.[1]

*[1]Instituto Politécnico Nacional -CICATA, Altamira; Km 14.5 Tampico-Puerto Industrial Highway, Altamira, Tamaulipas, P.C. 89600, México.*
*edonofre@ipn.mx*
*[2] CONACYT- Instituto Politécnico Nacional -CICATA, Altamira; Km 14.5 Tampico-Puerto Industrial Highway, Altamira, Tamaulipas, P.C. 89600, México.*
*[3]Centro Nacional de Investigaciones Metalúrgicas-CSIC; Gregorio del Amo avenue, 8, P.C. 28040 Madrid, Spain.*

## Abstract

Several authors have studied the thermal oxidation of Ti6Al4V, generating layers mainly TiO2 rutile phase in order to increase the wear and corrosion resistance. However, these layers have disadvantage of being susceptible to pitting corrosion. With the purpose to reduce its corrosion rate for its application as bone tissue replace implant, the coating system composed by $TiO_2$ thermally grown and $CeO_2$ formed by chemical conversion treatment is proposed taking advantage its characteristics as non-toxic antiseptic and anticorrosive.

In this work rutile structure was obtained on Ti6Al4V by quenching at 650 °C during 90 min followed by tempering at 450 °C. By cerium conversion treatments is formed a coating of cerium oxi-hydroxides, which films were characterized by X Ray Diffraction, Scanning Electronic Microscopy, X-Ray Photoelectronic Spectroscopy, Cyclic Polarization Curves, Electrochemical Impedance Spectroscopy and Scanning Electrochemical Microscope.

The preliminary results demonstrate that the coating system obtained reduces corrosion rate of the substrate. The TiO2 mainly work as a stable passive film and Cerium coating reduced the susceptibility to pitting corrosion

## Keywords

Biomaterial, coatings, thermal treatment, chemical conversion.

## Introduction

The biomaterials are artificial or natural materials, which are used in the implant fabrications, for replace the lost or sick biological structure and in this way restore its function [1]. The increased life expectancy in the population, degenerative diseases like arthritis (inflammation of the joints), osteoporosis (thinning of the bones), osteoarthritis (inflammation in the joints of the bones) and trauma lead to degradation of the bone mechanical properties due to the load or absence of normal biological self-healing, this has led to the dramatic increase in these implants and thereby increasing implantation surgery, replacement and revision of implants, which causes costs and pain to the wearer, so the development of new materials is necessary, especially for applications load bearing must possess excellent biocompatibility, resistance corrosion in the body environment, high wear resistance, high ductility and zero cytotoxicity[2]. Throughout nearly a century since the appearance of the first biomaterial [3] they have been studied materials searching these features.

Ti6Al4V alloy is considered exceptional biomaterial compared to other metals used for the same purposes as stainless steels, which have a lower corrosion resistance and a lower biocompatibility, because it can give off hexavalent chromium ions, which is carcinogenic. Other alloys used for the manufacture of implants are CoCrMo, however, because the chromium content, have the same disadvantage as stainless steels with respect to biocompatibility. Although being very hard, have very low mechanical properties so are usually used only for its low costs [4-6].

The Ti6Al4V has an elasticity closer to bone tissue than other alloys, also, naturally, titanium dioxide is formed in its surface, which has high corrosion resistance and porosity that promotes tissue adherence. However, the average life of a bone implant is approximately 10 years [8,9]; It is evident the need for development of alternative biomaterials to extend the useful life of the implant, thereby avoiding the replacement procedure of it.

For this purpose, a coating system of thermically formed titanium dioxide and cerium dioxide, which is a known effective anticorrosive, is proposed. As an added value dioxide of cerium has antiseptic properties, is a material that promotes cell growth, which will help the regeneration of the surrounding tissue and has self-healing capacity.

Therefore, in this research, the system of coatings obtained both by thermal treatment ($TiO_2$) and chemical conversion (CCT) on the Ti6Al4V alloy will be evaluated to determine the electrochemical behavior of the films formed in the presence of a physiological medium artificial, using electrochemical techniques.

## Experimental Methodology

The methodology consists of three stages: surfaces preparation, thermal treatment and chemical conversion treatment. After each of these steps, the samples were analyzed in order to confirm the presence of desired coatings and study its electrochemical behavior.

### Surface modification

Ti6Al4V cylindrical samples of 12.7 mm in diameter and 3 mm thick were used, which were roughed with carbide silicon sheets at different granulometry and polished to a mirror finish. The samples were thermically treated by tempered at 650 °C for 60 minutes and tempering at 450 ° C for 15 minutes to obtain a passive layer of $TiO_2$ in rutile phase; subsequently a chemical conversion treatment is performed.

Cerium oxide coatings were grow using $CeCl_3 \cdot 7H_2O$ (99.9%, Sigma-Aldrich) solutions of 0.001 M were used, and 3% v/v $H_2O_2$ solution was added to the chemical bath to accelerate the conversion process.

The identification structures present in the coating before and after thermal treatment was analyzed by X-Ray Diffraction. On the other hand, The samples corrosion rate were analyzed using by electrochemical impedance and the polarization curves, which was performed to obtain information about the corrosion mechanism and protective properties of the coating, The Electrochemical techniques were measured in a N302 Autolab bipotentiostat/galvanostat with respect to a saturated calomel electrode (Ag/AgCl) and graphite as an auxiliary electrode, while the working electrode was the sample Ti6Al4V, using as an electrolyte the PBS physiological media pH 6.8.

## Results and Discussion

Figure 1 illustrates the XRD patterns of the metallic substrate before and after quenching at 4 °C followed by tempering at 450 °C. The as-obtained substrate presented typical reflections, which match well those of titanium α and β phases (ICDD 44-1294 and 88-2321, respectively) [10,11]. This biphasic structure is characteristic for this type of alloys, where the amount of aluminium (6%) stabilises the α phase of titanium, while vanadium (4%) retains the β phase of titanium [12]. The XRD patterns of the thermally treated samples presented additional reflection peaks corresponded to the rutile phase of $TiO_2$ (ICDD 01-084-1284) [13]. Similar results have been previously reported when Ti6Al4V alloy was oxidised for long times during annealing [14]. Thus, XRD analysis demonstrated that the procedure proposed in this study allowed us to produce pure $TiO_2$ rutile phase, and the energy consumption was lower than those of the approaches commonly reported in the literature [14,15].

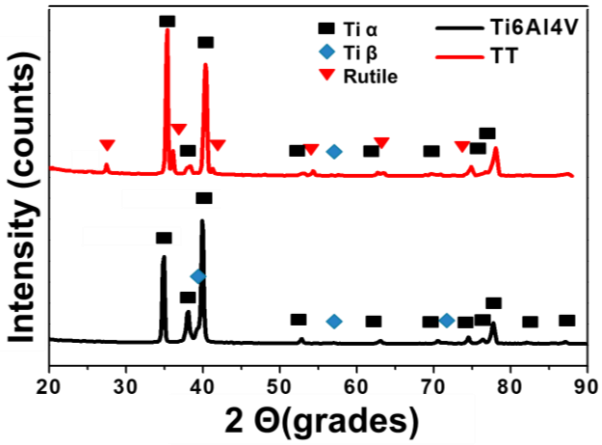


**Figure 1**. X-ray diffraction pattern of thermically treated Ti6Al4V.

Figures 2a-c present the SEM images (20 000× magnification) of the metallic substrates after thermal treatment (TT) at 650 °C and CCTs using the cerium concentration of 0.001 M. Some lines formed during the preparation of the substrate surfaces of the as-prepared samples (Figure 2a) while for the samples subjected to TT, the typical morphology of $TiO_2$ growth was observed (Figure 2b). The morphology consisted of small, semi-spherical particles, which agglomerated into aggregates featuring the average diameter of 48 nm. The differences in thickness of the $TiO_2$ layers between the quenched and non-treated samples were determined using cross-sectional SEM images (insets of Figure 2b). The average difference in thickness between the as-received and thermally treated substrates was 1 μm. On the other hand, the morphology of

the Ce coated sample obtained using the bath concentration of 0.001 M (which was used as reference) was smoother than that obtained after quenching the samples. These results were in agreement with those previously reported in the literature, where cerium oxide was deposited on $TiO_2$ films defects according to the mechanism described by Scholes et al. [16].

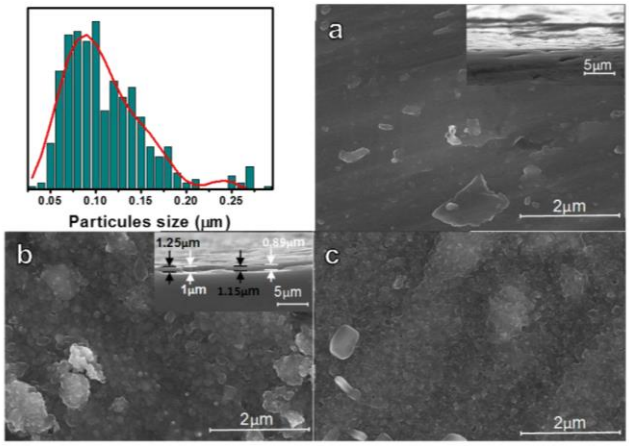


**Figure 2.** SEM micrographs of the samples: a) Ti6Al4V as-received state, b) Ti6Al4V thermally treated, transversal section and c) after treated at 0.001 M Ce.

Electrochemical measurements of the $CeO_2$-$TiO_2$-coated specimens were performed in acidic PBS solution (pH 6.8). The electrochemical behaviour of the metallic substrate before and after TT at 650 °C was also analysed. Samples were analysed using cyclic polarisation curves, and the results of the as-coated samples are presented in Figure 3 the corrosion current density of simple CCT 0.001 M, $i_{corr}$ (~$2.57 \times 10^{-7}$ A $cm^{-2}$), and voltage, $E_{corr}$ (0.46 $V_{Ag/AgCl}$), of all as-coated samples were identical.

.

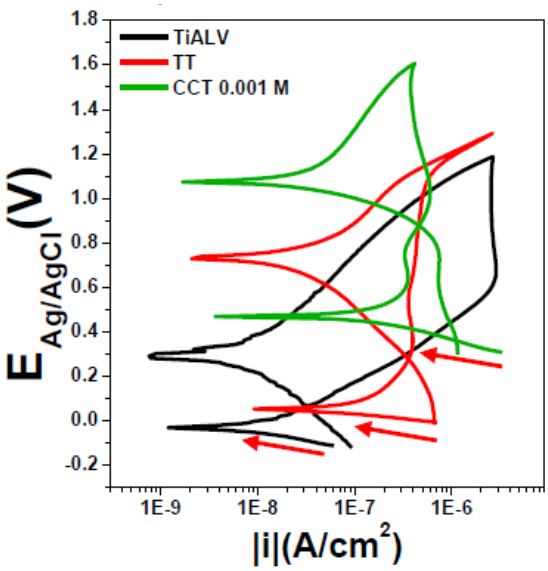


**Figure 3.** Cyclic polarization curves of TiAlV in PBS of samples a) treated at different bath concentrations and b) Ti6Al4V as-received state, thermal treatment (TT) and TT+ CCT 0.001 M.

The chemically treated samples presented a displacement of approximately 0.50 $V_{Ag/AgCl}$ towards positive values compared with the bare samples. Also, the $i_{corr}$ increased approximately one order of magnitude after TT and after the metallic substrate was chemically treated using cerium. These results were in agreement with the polarization resistance changes. However,

even if $i_{corr}$ increased, passivating films developed on the surfaces of the samples that were chemically treated using cerium at 0.66 $V_{Ag/AgCl}$, and their $i_{corr}$ values remained almost stable after 1.0 $V_{Ag/AgCl}$. This delayed the pitting potential and passivating current ($3.54 \times 10^{-7}$ A $cm^{-2}$) even after 1.6 $V_{Ag/AgCl}$. On the contrary, a quasisteady- state was observed when the samples that underwent TT were evaluated in PBS solution, where the corrosion potential was approximately 0.050 $V_{Ag/AgCl}$ and pseudopassivating films were observed in the potential range of 0.32-1.080 $V_{Ag/AgCl}$ at the average passivating current of approximately $3.95 \times 10^{-7}$ A $cm^{-2}$. The $i_{corr}$ values increased significantly at higher potential values. When exposed to harsh media, the bare samples presented typical active behaviour, and passivating compounds formed in the range of 0.66- 1.18 $V_{Ag/AgCl}$. However, in this case, the passivation current density, $i_{pass}$, was approximately $2.85 \times 10^{-6}$ A $cm^{-2}$. The reverse cycles of all samples indicated irreversible processes and potential and current values which were dependent of the surface treatment. However, at 1.080 $V_{Ag/AgCl}$ (1.056 $V_{SHE}$, where SHE is the standard hydrogen electrode) the increase in $i_{pass}$ suggested that a localised corrosion process occurred, which was metastable during reverse polarisation. According to the theory established by Burstein et al. [17], metastable pits grow under diffusion control. The growth of pitting requires the development of extremely harsh environments within it. Once samples are removed from the harsh environment, re-passivation occurs. This phenomenon was not observed for the samples subjected to CCT, where two passivation zones were observed in the potential range of ~1 V, which suggested the presence of two different types of cerium oxides/hydroxides. The first passivation zone was related to $Ce^{+3}$, and was interrupted at 0.800 $V_{Ag/AgCl}$ owing to the slight increase in current intensity. This increase in intensity was attributed to the $Ce^{+3} \rightarrow Ce^{+4}$ reaction, which occurred during anodic polarisation and led to the formation of the second passivation zone, which was related to cerium (IV) hydroxide.

This behaviour was attributed to anodic polarisation favouring a superficial reaction, where he CCT by-products, which contained $Ce^{+3}$ ions, converted into $Ce^{+4}$-containing products. Figure 4 presents the EIS curves and their fitting for film grew onto Ti6Al4V substrates using CCT. The equivalent circuits used during fitting are also illustrated in the inset, and the results are displayed in Table 4. The electrochemical response of the coated samples was simulated using a typical [$R_s$ ($CPE_1$ ($R_1$ ($CPE_2$ ($R_2$ $W_{o1}$)))] circuit, where $R_s$ is the solution resistance, and $R_1$ and $R_2$ are the coating and charge transfer resistances, respectively. Capacitances were simulated as constant phase elements (CPEs), which were used to simulate the deformation of the semicircle owing to heterogeneities, such as roughness of the coating surface [18].

Lastly, diffusion was observed at low frequency regions (~45°) and was adjusted in the equivalent circuit using a finite Warburg element. The diffusion impedance in a thin layer cell is theoretically expressed as where, $R_d$ is the scaling factor, and $Z_M$ indicates the diffusion of species, typicallyvthe transport of ions through the oxide [19].

The solution resistance of all samples in PBS was approximately 82 Ω. As stated above, the resistance polarisation values of samples were similar, independent of the cerium concentration used for the CCT, but it decreased to 27% as the cerium bath concentration increased, which confirmed that low cerium amounts favoured the formation of more resistive films. Thus, the two-time constants, at high and intermediate frequencies, were associated with the coating process, which was followed by a controlled diffusion process.

The simulation values remained practically constant, and were independent of the concentration of the cerium baths used for CCT. These findings were in good agreement with the results previously reported in the literature for another type of substrate [20]. The EIS spectra of the

cerium coated specimens using the 0.001 M cerium bath were compared with those of the thermally treated and bare sample. The electrochemical performance of the Ti6Al4V substrates was simulated using a Randles circuit, and the solution resistance (Rs) was again approximately 82 Ω. The ideal admittance was 2.9E-5 (S $s_n$ $cm^{-2}$). This capacitance was almost pure, its n value was 0.92, while the charge transfer resistance ($R_1$) was 6.9 E5 Ω $cm^2$. The fitting of the samples subjected to TT was achieved using the equivalent circuit depicted in the inset of the Nyquist plots.The equivalent circuit considers a time constant at high frequencies associated with $TiO_2$ film followed to a Warburg element (W) (diffusion process), and at low frequencies shows a time constant related with the metastable pits that are produced during evaluation.

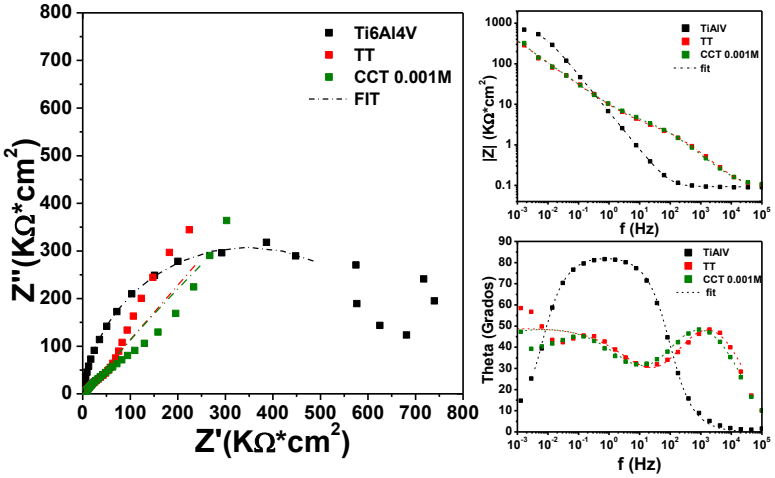


**Figure 4.** Impedance spectra measured in PBS pH 6.4, of Ti6Al4V bare, samples thermally treated (TT) and after CCTs using a bath concentration of 0.001 M.

Figure 8 illustrates the potential maps obtained using the Kelvin probe for the scanned area of 3000 × 3000 μm at t = 0, 12, and 24 h. The surface potential was fairly constant in time for the chemically treated samples, which suggested that cerium conversion coatings were grown uniformly over the substrate surface and were stable under experimental conditions (90% RH). However, the average potential value of the as-received material was 112 $mV_{SHE}$ and varied by ± 36 $mV_{SHE}$ after TT. Moreover, the potential increased to 511 ± 28 $mV_{SHE}$, i.e. the potential shifted by approximately 400 mV towards positive values, and after CCT the potential was displaced by approximately 600 $mV_{SHE}$ with respect to that of the bare Ti6Al4V sample. Since the potential of the samples obtained using different cerium concentrations presented variations of ± 25 mV and remained relatively constant in time, it was concluded that low cerium concentrations were sufficient to obtain protective films.

Lastly, to prove these assumption, current maps of the same surfaces were obtained using SECM measurements at t = 0 h and the results are presented in Figure 5. The intensity of the current for the bare Ti6Al4V sample (Figure 5a) ranged from 0.29 to 0.51 nA, and the shape of the current map suggested that the surface was not completely homogeneous since it presented a large area of greater current intensity. The current of the thermally treated samples (Figure 5b) was reduced, and ranged from 0.11 to 0.4 nA, which suggested that the surfaces of these samples were less active. However, small fluctuations in current were observed at some points, and those could be related to the presence of unstable pores (very small active nuclei) that were re-passivated or plugged. The samples that underwent CCT using cerium concentrations of 0.001 M (Figure c) exhibited similar current maps, and featured variations in the range of 0.24 to 0.80 nA, which were higher than those of the bare or thermally treated Ti6Al4V samples. The increase in current might have been due to the aforementioned surface reaction ($Ce^{3+}$ →

$Ce^{4+}$ + 1e-). Ti6Al4V implants suffer from pitting corrosion, which is disadvantageous. Cerium oxide deposited using CCT was effective for hindering localised corrosion, within the scope of this study, as well as according to research performed by other scholars on materials such as stainless steel [21], magnesium [22] and aluminium alloys [23]. This was attributed to the affinity of cerium oxide for cathodic zones [24] owing to the reduction of $H_2O_2$ or $O_2$ at the surface, which generated $OH^-$ ions, which could later react with cerium species. In addition to providing further benefits for implant preservation, these coatings also helped regenerate and protect the surrounding tissues.

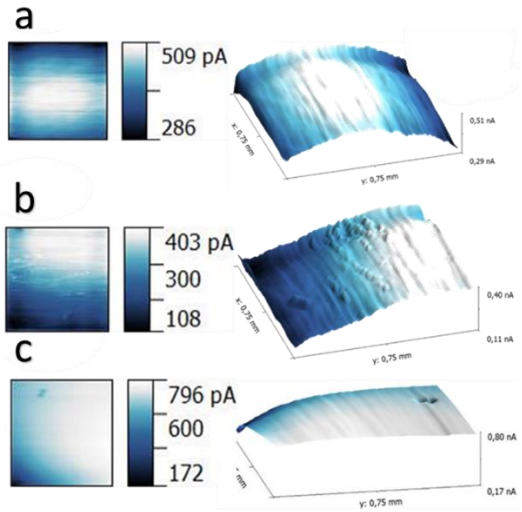


**Figure 5.** Current intensity maps obtained by SECM of the samples Ti6Al4V (a), TT (b), and CCT 0.001M (c).

## Conclusions

The XRD patterns indicated that $TiO_2$ rutile phase films grew on the surface of the as received Ti6Al4V substrates after they underwent TT at 650 °C. The observed reflections were still present even after the samples were subjected to CCT using cerium, which could be explained in terms of the detection limit of the XRD technique. The chemical composition of the Ce/$TiO_2$/Ti6Al4V systems confirmed that the conversion films consisted of $Ce^{3+}$ and $Ce^{4+}$ oxides/hydroxides, and their formation apparently followed the mechanism proposed by Hinton. The roughness of these coatings was lower than that of other materials used for implants, but these coated materials were deemed appropriate for use as implants in areas such as the skull and spine where bacterial resistance is critical.

Electrochemical evaluation demonstrated that the $TiO_2$ formed after TT functioned as passivation film, which increased the corrosion resistance of the substrate. However, the $TiO_2$ layer exhibited localised corrosion in metastable pitting form. Pitting corrosion was reduced using cerium CCT, which addressed one of the main shortcomings of Ti6Al4V.

## References

1. R. Deshmukh and . S. Kulkarni, IJCET, **5** (2015) 4.
2. M. Geetha , A. Singh , R. Asokamani and A. Gogia, Prog. Mater. Sci., **54** (2009).
3. E. Mateus , Metalurgia actual, **26** (2012).

4. M. Ahmed, J. Byrne, T. Keyes, W. Ahmed, A. Elhissi, and M. Jackson, The Design and Manufacture of Medical Devices, **1** (2012).
5. B. Baumann, J. Seufert , F. Jakob, U. Nöth, O. Rolf, J. Eulert, C. Rader, J Orthop Res, **23** (2006) 6.
6. A. Echavarría, Revista Facultad de Ingeniería Universidad de Antioquia, **30** (2003).
7. R. Sharmila, N. Selvakumar and K. Jeyasubramania, Mater. Lett., **91** (2013).
8. G. Gajski, z. Jelčić, V. Oreščanin, M. Gerić and V. Garaj-Vrhovac, Biochim Biophys Acta **Gen** Subj., **1** (2014) 1840.
9. D. Granchi, E. Cenni, G. Trisolino, A. Giunti and N. Baldini, J. Biomed. Mater. Res. **B**, **77** (2005) 2.
10. R. Sailer and G. McCarthy, ICDD grant-in-aid. Fargo, North Dakota, USA: North Dakota State University (1993).
11. J. Haglund, F. Fernandez, G. Grimvall, Haglund, J., Fernandez-Guillermet, F., Grimvall, G., Korling, M., Phys. Rev. B. Condens. Matter, **48** (1993)11685.
12. L. Córdoba, Relación entre microestructura y resistencia a corrosión de la aleación biocompatible Ti6Al4V deformada en caliente, Colombia: Universidad Nacional de Colombia Facultad de Minas (2009).
13. J. Burdett, T. Hughbanks, G. Miller, J. Richardson and J. Smith, J. Am. Chem. Soc. **109** (1987) 3639.
14. H. Guleryuz and H. Cimenoglu, J. Alloys Compd., **472** (2009) 241.
15. S. Kumar, T. Sankara N., S. Sundara R. and S. Seshad, Mater. Charact., **61** (2010) 589.
16. F. H. Scholes, C. Soste, A. E. Hughes, S. G. Hardin and P. R. Curtis, Appl. Surf. Sci., **253** (2006) 1770.
17. T. Li, L. Liu, B. Zhang, Y. Li and F. Wang, Corros. Sci., 1(2017).
18. M. A. Dominguez, E. Ramírez, A. M. Torres, V. Garibay-Febles, K. Philippot, Int. J. Hydrogen Energy, **37** (2012) 6
19. V. S. Simi and N. Rajendran, Mater. Charact., **129** (2017) 67.
20. A. Decroly and J. Petitjean, Surf. Coat. Technol., **194** (2005) 1.
21. C. Wang, F. Jiang and F. Wang, Corros. Sci., **46** (2004) 75.
22. M. Dabalà, K. Brunelli, E. Napol, M. Magrinia, Surf Coat Tech, **172** (2003) 227.
23. C. Wang, F. Jiang, F. Wang, Corrosion, vol. 60, no. 3, pp. 237-243, 2004.
24. M. Dabalà, L. Armela, A. Buchberge and I. Calliari, Appl Surf Sci., **172** (2001) 3.